A DVBH/GSM/UMTS Planar Antenna for Multimode Wireless Devices

Leonardo Lizzi, Federico Viani, Edoardo Zeni, and Andrea Massa, *Member, IEEE*

***Abstract*—In this letter, the prototype of a planar antenna working in three different frequency bands and suitable to be integrated in multimode wireless devices is described. The antenna is fed by a single RF port without any matching circuit, and it operates in a DVBH channel and at GSM and UMTS frequency bands. Its dimension is of 0.15λ at the lower frequency band. The effectiveness and feasibility of the proposed antenna is assessed by means of both simulations and measurements.**

***Index Terms*—DVBH, fractal antennas, GSM, multiband, multimode, UMTS.**

I. Introduction

TODAY'S competitive market requires multimode capabilities for each wireless device because of the rising demand for new, higher speed mobile broadband and multifunction applications. On the other hand, mobile handsets are characterized by smaller and smaller sizes and reduced weights thanks to the progress of modern integrating circuit technology and following the users' needs. To this end, the design of suitable RF front-ends plays a very important and critical role.

Concerning the dimension requirement, the use of conventional monopole-like antennas is generally avoided because of their relatively large sizes when compared to that of the device itself [1]. A more effective solution considers microstrip planar radiators, which are more easily adaptable to the shape of the handset at hand. However, standard half-wavelength microstrip antennas at the operating frequencies of modern mobile applications (e.g., DVBH) turn out to be still too large for an efficient integration into a miniaturized mobile device.

With regards to the multiband operation [2], new strategies are under development for integrating multiple functionalities and reducing, at the same time, both costs and complexity. Such a task is usually addressed by using duplexers along with bandpass filters in the receiving and transmitting paths. Unfortunately, such a solution needs surface acoustic wave (SAW) filters and low noise amplifiers (LNAs) with a nonnegligible increase of the costs and dimensions. Some attempts to minimize the occupied space have been done by integrating the LNA on-chip. Nevertheless, further efforts are devoted to avoid the use of external filters in order to reduce the number of components and to simplify the board layout. Toward this end, a possible solution consists of moving the frequency selectivity functions "closer" to the antenna. In other words, this means that the radiating system must show an adequate impedance matching within each band of operation without external components.

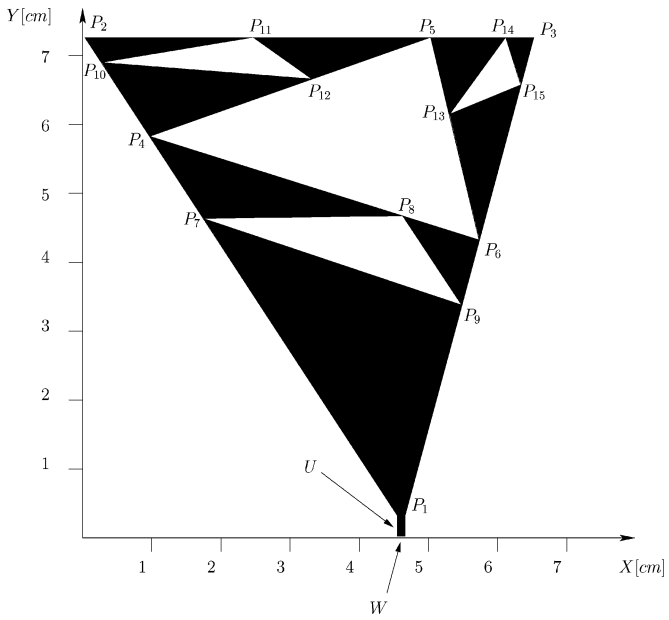

Fig. 1. Geometry of the multimode three-band antenna.

Following such a guideline, this letter describes a three-band fractal antenna synthesized by exploiting the optimization approach proposed in [3] and [4] and aimed at minimizing the radiator dimensions as well as at obtaining a multiband behavior. The result is a single radiating structure that resonates at three different bands and is suitable for an integration in board layouts. As a matter of fact, it should be pointed out that fractal-shaped antennas have proven to be effective not only for miniaturization purposes [5], but also to achieve a multiband behavior [6]–[9] since their radiation properties are determined by the electrodynamic properties of fractal shapes.

The outline of this letter is as follows. Section II describes the antenna geometry and some details on the design procedure. The efficiency and reliability of the synthesized antenna are assessed in Section III by means of both numerical and experimental results. Finally, some concluding remarks are given in Section IV.

II. Antenna Design

The geometry of the antenna is shown in Fig. 1. As it can be observed, the reference shape is a planar Sierpinski prefractal,

Manuscript received February 25, 2009; revised April 05, 2009. First published May 15, 2009; current version published July 01, 2009.

The authors are with the Department of Information Engineering and Computer Science, University of Trento, Trento, Italy (e-mail: leonardo.lizzi@disi.unitn.it; federico.viani@disi.unitn.it; edoardo.zeni@disi.unitn.it; andrea.massa@ing.unitn.it).

Color versions of one or more of the figures in this letter are available online at http://ieeexplore.ieee.org.

Digital Object Identifier 10.1109/LAWP.2009.2022962

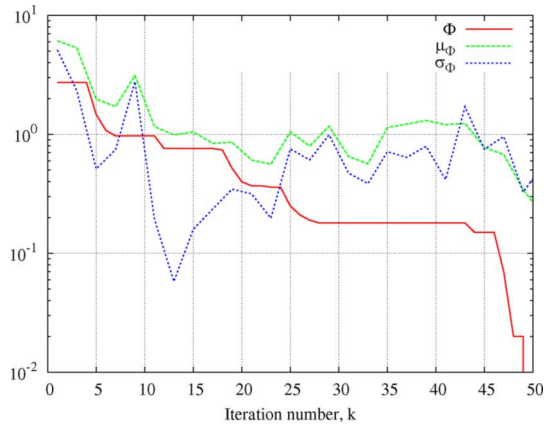

Fig. 2. Behaviors of the cost function statistics during the iterative PSO optimization.

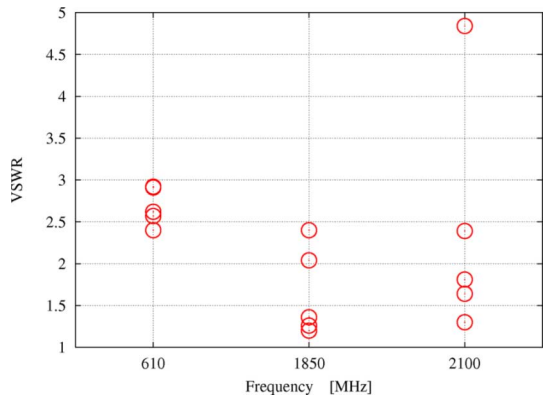

Fig. 3. Simulated VSWR values, at the center of each frequency band, for the trial solutions at the convergence.

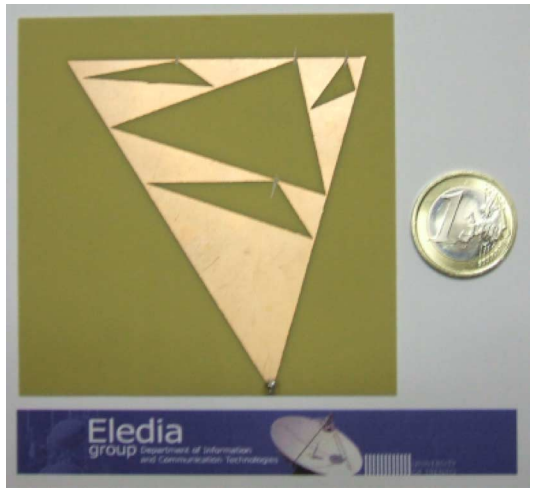

Fig. 4. Antenna prototype.

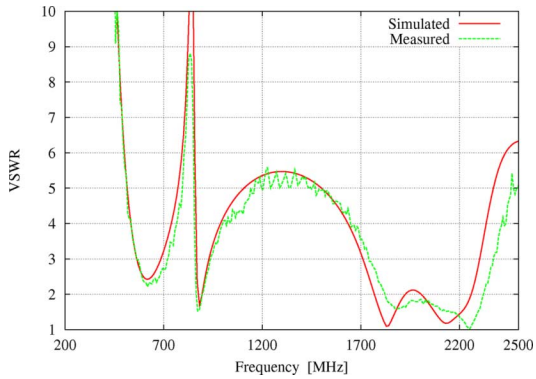

Fig. 5. Simulated and measured VSWR values.

where three iteration stages ($s = 0, 1, 2$) have been considered to set three different resonances [7]. From a geometric point of view, the antenna structure is uniquely defined by the following descriptors:

$$\chi = \{U, W, P_i = (X_i, Y_i)\,;\, i = 1, \ldots, 15\} \qquad (1)$$

where U and W are the length and the width of the input section, respectively. Moreover, (X_i, Y_i) $i = 1, \ldots, 15$ are the coordinates of the vertexes of the void triangles in Fig. 1 descriptive of the antenna geometry.

Since the antenna is required to be compact (maximum size 8×8 [cm^2]) and to simultaneously operate at three different frequency bands, the user-defined constraints require voltage standing wave ratio (VSWR) values lower than 2.5 at the center of each frequency band and smaller than 3.0 along the whole bandwidths, respectively. With regards to the synthesis process, the final antenna shape has then been determined by applying the optimization procedure proposed in [3] and [4]. Such an iterative technique integrates an electromagnetic simulator based on the method of moments (MoM) [10] and a particle swarm optimizer (PSO) [11], [12] in order to find an antenna configuration fitting a set of user-defined constraints on the size and the impedance-matching behavior. In more detail, a swarm of $R = 5$ particles has been randomly initialized and iteratively updated according to the PSO logic until a solution fitting the user-defined requirements has been found. In Fig. 2, the behavior of the cost function Φ over the iterations ($k_{\text{conv}} = 50$) is given. For completeness, the cost function mean value μ_Φ as well as the standard deviation σ_Φ are reported. With regards to the optimization results, Fig. 3 shows a scatter plot of the VSWR values at k_{conv}. Each point of the plot indicates the simulated VSWR value at the center of a frequency band in correspondence with a swarm solution. As it can be observed, all the trial solutions at the convergence meet the performance requirements in the GSM and UMTS bands, but only one representative point (i.e., only one trial solution) falls below $\text{VSWR} = 2.5$ in the DVBH band.

TABLE I
SIMULATED PERFORMANCES

Wireless Service	Frequency Band $[MHz]$	VSWR Centerband	VSWR on Band
DVBH	$606 \div 614$	2.4	2.5
GSM	$1800 \div 1900$	1.2	1.8
UMTS	$2000 \div 2200$	1.3	1.9

Taking into account the constraints on the shape and electric behavior of the device at hand, the following values of the antenna descriptors have been identified at the end of the PSO-based optimization process. The dimensions of the input section turns out to be $U = 0.28$ mm and $W = 0.12$ mm. Moreover, the coordinates of the control points (in [cm]) result: $P_1 =$

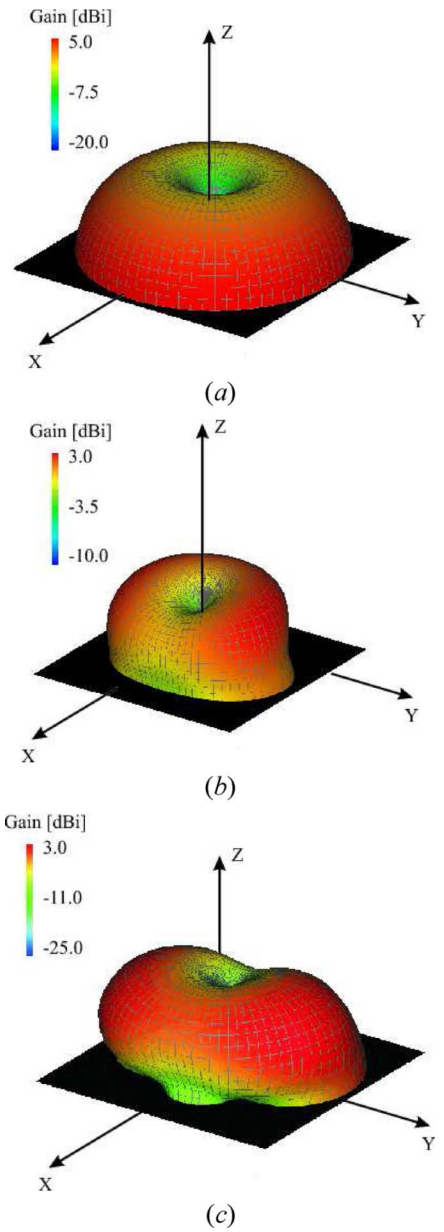

Fig. 6. Simulated 3D radiation patterns. (a) Total gain at $f_0^{\mathrm{DVBH}} = 610$ MHz. (b) Total gain at $f_0^{\mathrm{GSM1800}} = 1850$ MHz. (c) Total gain at $f_0^{\mathrm{UMTS}} = 2100$ MHz.

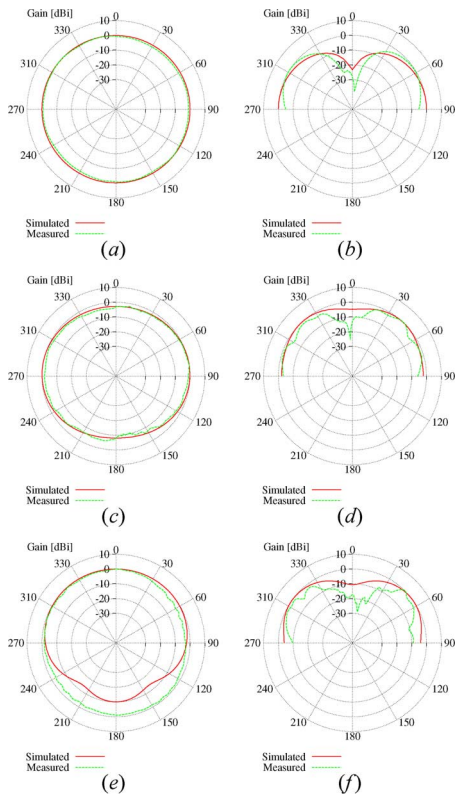

Fig. 7. Simulated and measured radiation patterns. (a) Horizontal plane ($\theta = 90°$) at $f_0^{\mathrm{DVBH}} = 610$ MHz. (b) Vertical plane ($\phi = 90°$) at $f_0^{\mathrm{DVBH}} = 610$ MHz. (c) Horizontal plane ($\theta = 90°$) at $f_0^{\mathrm{GSM1800}} = 1850$ MHz. (d) Vertical plane ($\phi = 90°$) at $f_0^{\mathrm{GSM1800}} = 1850$ MHz. (e) Horizontal plane ($\theta = 90°$) at $f_0^{\mathrm{UMTS}} = 2100$ MHz. (f) Vertical plane ($\phi = 90°$) at $f_0^{\mathrm{UMTS}} = 2100$ MHz.

$(4.5, 0.1)$, $P_2 = (0.0, 7.4)$, $P_3 = (6.6, 7.4)$, $P_4 = (1.0, 5.8)$, $P_5 = (5.2, 7.4)$, $P_6 = (5.8, 4.3)$, $P_7 = (1.8, 4.7)$, $P_8 = (4.7, 4.7)$, $P_9 = (5.5, 3.4)$, $P_{10} = (0.3, 7.0)$, $P_{11} = (2.5, 7.4)$, $P_{12} = (3.3, 6.7)$, $P_{13} = (5.4, 6.2)$, $P_{14} = (6.2, 7.4)$, and $P_{15} = (6.4, 6.7)$. As a macroscopic result, the antenna prototype covers an area of 6.6×7.4 cm^2. More specifically, the maximum linear dimension of the antenna at the highest wavelength of operation is equal to 0.15λ, with a reduction of more than 40% with respect to the corresponding quarter-wave resonant monopole.

III. Numerical and Experimental Results

In this section, some numerical and experimental results aimed at validating the efficiency and reliability of the proposed antenna are shown. To perform the experimental measurements, a prototype of the antenna has been built (Fig. 4) on a planar dielectric substrate (Arlon: thickness $h = 0.8$ mm, relative permittivity $\varepsilon_r = 3.38$, $\tan\delta = 0.002$ at $f = 10$ GHz). The prototype, fed by a single 50-Ω RF port connected to the antenna structure in P_1 and mounted on a metallic ground plane, has been used to collect both VSWR and radiation patterns measurements in an anechoic chamber.

The electric performances of the synthesized antenna are summarized in Table I. As far as the impedance matching is concerned, Fig. 5 shows a comparison between measured and simulated VSWR values. As expected, the antenna resonances are located at the center of a DVBH channel ($f_0^{\mathrm{DVBH}} = 610$ MHz), in the higher GSM band ($f_0^{\mathrm{GSM1800}} = 1850$ MHz), and in correspondence with the UMTS band ($f_0^{\mathrm{UMTS}} = 2100$ MHz). Besides the good agreement between the two plots (i.e., numerical and measured values), the antenna shows a good impedance matching in the GSM band ($1.2 \leq \mathrm{VSWR}_{\mathrm{simulated}}^{\mathrm{GSM1800}} \leq 1.8$, $1.6 \leq \mathrm{VSWR}_{\mathrm{measured}}^{\mathrm{GSM1800}} \leq 2.1$) and in the UMTS band ($1.3 \leq \mathrm{VSWR}_{\mathrm{simulated}}^{\mathrm{UMTS}} \leq 1.9$, $1.3 \leq \mathrm{VSWR}_{\mathrm{measured}}^{\mathrm{UMTS}} \leq 1.8$). On the other hand, an acceptable matching has also been obtained at the lowest working frequency devoted to the reception of a DVBH channel ($2.4 \leq \mathrm{VSWR}_{\mathrm{simulated}}^{\mathrm{DVBH}} \leq 2.5$, $2.2 \leq \mathrm{VSWR}_{\mathrm{measured}}^{\mathrm{DVBH}} \leq 2.3$). Higher VSWR values in this latter band are mainly caused by the constraint on the antenna size. As a matter of fact, a VSWR value below 2:1 can be easily

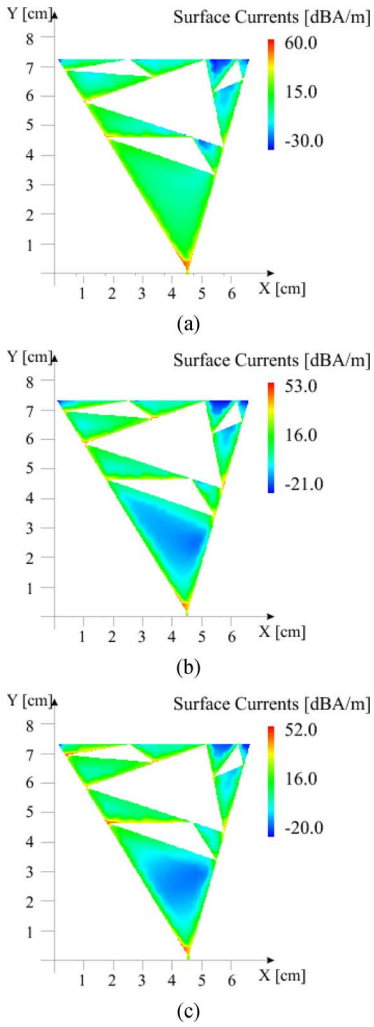

Fig. 8. Simulated surface currents at (a) $f_0^{\mathrm{DVBH}} = 610$ MHz, (b) $f_0^{\mathrm{GSM1800}} = 1850$ MHz, and (*c*) $f_0^{\mathrm{UMTS}} = 2100$ MHz.

reached by relaxing the miniaturization requirement (e.g., from 8×8 to 9.5×9.5 [cm^2]).

With regards to the radiation properties, Fig. 6 shows the simulated three-dimensional gain patterns computed at the center of each frequency band. As it can be observed, the radiation pattern is monopole-like at the lowest frequency [Fig. 6(a)], while some variations occur when the working frequency increases [Fig. 6(b)-(c)]. As a matter of fact, the antenna tends to work like a half-wave monopole in the highest frequency bands. Such a behavior is further pointed out by the appearance of additional lobes in the radiation diagram. Nevertheless, the omnidirectional behavior along the horizontal plane makes the antenna suitable for mobile wireless devices.

For completeness, the numerical values are compared to the measurements at the horizontal plane ($\theta = 90°$) and at the vertical one ($\phi = 90°$) (Fig. 7). Once again, measurements and simulations turn out to be in good agreement, although some difference are present in the UMTS band [Fig. 7(e)-(f)]. They can be ascribed to the nonideal behavior of the measurement environment at higher frequencies.

Finally, the simulated behaviors of the surface currents are shown in Fig. 8. As expected, and because of the multiband operation, the plots at the different frequencies significantly differ. Moreover, the variations of the surface current along the longitudinal direction show a trend similar to that of a quarter-wave monopole in the DVBH band [Fig. 8(a)], while they turn out to be close to that of a half-wave monopole at the higher working frequencies [Fig. 8(b)-(c)].

IV. Conclusion

A three-band planar antenna for DVBH, GSM, and UMTS wireless services has been described. The antenna exhibits reduced dimensions and an acceptable impedance matching in the working frequency bands. The antenna performances have been numerically and experimentally assessed. The obtained results confirm the reliability of the numerical synthesis as well as the feasibility and effectiveness of the proposed solution for multifunction wireless devices.

References

[1] Y.-X. Guo, M. Y. W. Chia, and Z. N. Chen, "Miniature built-in multiband antennas for mobile handsets," *IEEE Trans. Antennas Propag.*, vol. 52, no. 8, pp. 1936–1944, Aug. 2004.

[2] M. Martinez-Vazquez, O. Litschke, M. Geissler, D. Heberling, A. M. Martinez-Gonzalez, and D. Sanchez-Hernandez, "Integrated planar multiband antennas for personal communication handsets," *IEEE Trans. Antennas Propag.*, vol. 54, no. 2, pt. 1, pp. 384–391, Feb. 2006.

[3] R. Azaro, G. Boato, M. Donelli, and A. Massa, "Design of a prefractal monopolar anenna for 3.4–3.6 GHz Wi-Max band portable devices," *IEEE Antennas Wireless Propag. Lett.*, vol. 5, pp. 116–119, 2006.

[4] R. Azaro, F. De Natale, M. Donelli, E. Zeni, and A. Massa, "Synthesis of a prefractal dual-band monopolar antenna for GPS applications," *IEEE Antennas Wireless Propag. Lett.*, vol. 5, pp. 361–364, 2006.

[5] J. Gianvittorio and Y. Rahmat-Samii, "Fractal antennas: A novel antenna miniaturization technique, and applications," *IEEE Antennas Propag. Mag.*, vol. 44, no. 1, pp. 20–36, Feb. 2002.

[6] D. H. Werner, P. L. Werner, and K. H. Church, "Genetically engineered multiband fractal antennas," *Electron. Lett.*, vol. 37, pp. 1150–1151, 2001.

[7] C. Puente-Baliarda, J. Romeu, R. Pous, and A. Cardama, "On the behavior of the Sierpinski multiband fractal antenna," *IEEE Trans. Antennas Propag.*, vol. 46, no. 4, pp. 517–524, Apr. 1998.

[8] D. H. Werner and S. Ganguly, "An overview of fractal antenna engineering research," *IEEE Antennas Propag. Mag.*, vol. 45, no. 1, pp. 38–57, Feb. 2003.

[9] D. H. Werner and R. Mittra, *Frontiers in Electromagnetics*. Piscataway, NJ: IEEE Press, 2000.

[10] R. F. Harrington, *Field Computation by Moment Methods*. Malabar, FL: Krieger, 1987.

[11] J. Robinson and Y. Rahmat-Samii, "Particle swarm optimization in electromagnetics," *IEEE Trans. Antennas Propag.*, vol. 52, no. 2, pp. 397–407, Feb. 2004.

[12] D. W. Boeringer and D. H. Werner, "Particle swarm optimization versus genetic algorithms for phased arrays synthesis," *IEEE Trans. Antennas Propag.*, vol. 52, no. 3, pp. 771–779, Mar. 2004.